Available online at www.sciencedirect.com

ScienceDirect

Procedia Structural Integrity 23 (2019) 197–202

Structural Integrity Procedia

www.elsevier.com/locate/procedia

9th International Conference on Materials Structure and Micromechanics of Fracture

Interaction of fatigue and creep in MAR-M 247 superalloy

Vít Horník[a,b,*], Stanislava Fintová[a,c], Miroslav Šmíd[a], Pavel Hutař[a,c], Karel Hrbáček[d], Ludvík Kunz[a]

[a]*Institute of Physics of Materials, AS CR, Žižkova 22, Brno, 616 62, Czech Republic*
[b]*Brno University of Technology, Technická 2896/2, Brno 616 69, Czech Republic*
[c]*CEITEC IPM, Žižkova 22, Brno, 616 62, Czech Republic*
[d]*PBS Velká Bíteš, a. s., Vlkovská 279, Velká Bíteš, 595 12, Czech Republic*

Abstract

Lifetime of MAR-M 247 Ni-based superalloy was experimentally studied under high-frequency cyclic loading (120 Hz) with constant tensile mean stress $\sigma_m = 300$ MPa at temperature 900 °C in air. The stress amplitude σ_a was changed in order to investigate the superalloy lifetime in a wide range of conditions, from pure creep to pure fatigue. The superposition of the stress amplitude on the mean stress does not influence the specimen lifetime until a threshold value is reached. Scanning electron microscopy was utilized for the fracture surface observation with the aim to identify the governing damage mechanisms for particular test conditions.

Keywords: creep/fatigue interaction, superalloy; MAR-M 247; high temperature.

1. Introduction

Cast Ni-based superalloys are structural materials for high-temperature applications, especially in automotive and energy industry. This class of alloys is widely used for components, for instance, turbine blades and turbochargers, which are exposed to high temperatures and/or significant thermal gradients, centrifugal forces and high-frequency

* Corresponding author.
E-mail address: hornik@ipm.cz

10.1016/j.prostr.2020.01.086

vibrations, e.g. Reed (2008). Therefore, the creep and fatigue damage mechanisms and their interaction determine the service life of components under these loading conditions.

The influence of low cycle fatigue and creep loading (namely dwell periods) on the high-temperature fatigue behavior and lifetime of superalloys has been published in numerous papers, e.g. Šulák et al. (2017), Beck et al. (2002) and Goswami and Hannien (2001). On the other hand, the knowledge on the influence of high-frequency fatigue superimposed on mean stress at high temperature on the lifetime and analysis of damage mechanisms are nearly missing in the open literature. Lukáš et al. (1997) presented the study performed on CMSX-4 single crystal superalloy, where high-frequency (90 - 95 Hz) stress amplitude σ_a superimposed on mean stress σ_m at 800 °C was shown to reduce the creep damage process, however, it accelerates the fatigue damage of material. Studies carried out on cast polycrystalline superalloys do not report any reduction of time to fracture t_f while superimposing small amplitudes with frequencies around 120 Hz at the temperature 800 °C in the case of IN 713LC and at 900 °C for MAR-M 247, e.g. Horník et al. (2017), Kunz et al. (2017).

This study aims to identify the creep and fatigue damage mechanism and its effect on the crack initiation and propagation in MAR-M 247 nickel-based superalloy. The creep/fatigue tests, upon constant mean stress and a wide range of stress amplitudes, were carried out to evaluate the effect of the stress amplitude on the specimen lifetime.

2. Material

The polycrystalline MAR-M 247 superalloy was provided by PBS Velká Bíteš company in a form of pre-cast rods. The chemical composition of the studied alloy is shown in Table 1. The pouring temperature into the mold was 1360 ± 10 °C. The cast semi-products were processed by hot isostatic pressing (HIP) at the temperature 1200 °C and pressure 100 MPa for 4 hours followed by two steps heat treatment consisting in solution annealing at the temperature 1200 °C for 2 hours with cooling on the air and precipitation annealing at the temperature 870 °C for 24 hours with cooling on the air. The final structure of the processed material is a coarse dendritic structure with an average grain size about 2.5 mm (measured by the linear intercept method on 10 different areas of the microstructure), Fig. 1. The volume fraction of precipitates γ', around 60 %, was determined from 10 scanning electron micrographs. Besides precipitates γ' and matrix γ, the microstructure consists of eutectics γ / γ' and numerous carbides along grain boundaries and interdendritic areas. The morphology of the strengthening precipitates γ' is heterogeneous, fine cuboidal (edge size of ~ 0.4 μm) and coarse spherical (~ 1.6 μm in diameter) shape. The casting defects were not observed in the material microstructure.

The creep/fatigue tests were performed on resonant testing machine Amsler with 100 kN force range under load control regime. The specimens were heated at the testing temperature 900 °C by an electric resistance furnace on air. The temperature of testing was held with long-term stability ± 1 °C, controlled by two thermocouples. Mean stress σ_m = 300 MPa was applied for creep and creep/fatigue tests. The frequency of cyclic loading was about 120 Hz. Cylindrical test specimens with a geometry shown in Fig. 2 were used for the purposes of this study. Gauge length of all specimens was mechanically ground. The surface of fractured specimens was examined by TESCAN Lyra3 XMU scanning electron microscope (SEM).

Table 1. Chemical composition of MAR-M 247 (in wt %), given by producer.

C	Cr	W	Co	Al	Ti	Ta	Hf	Mo	Nb	B	Zr	Ni
0.15	8.50	9.85	9.77	5.50	1.02	3.01	1.31	0.74	0.05	0.015	0.037	bal.

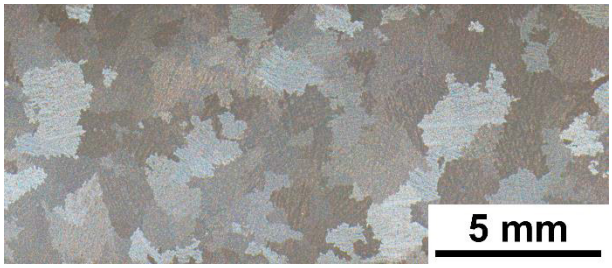

Fig. 1. Coarse dendritic structure of MAR-M 247.

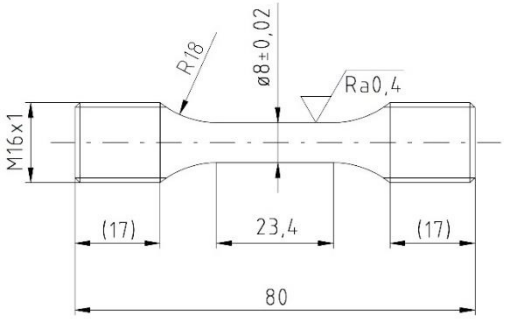

Fig. 2. Schematic of specimen geometry.

3. Results and discussion

Experimentally determined dependence of the time to fracture t_f on high-frequency stress amplitude σ_a superimposed on mean stress σ_m = 300 MPa at temperature 900 °C is shown in Fig. 3. Superimposition of small stress amplitudes does not influence the MAR-M 247 lifetime until the stress amplitude reaches a certain threshold value. The dependence in Fig. 3 indicates that the threshold value is of about 60 MPa. Imposing higher stress amplitudes results in a decrease of specimen lifetime. In order to clarify this phenomenon, the fractographic analysis was carried out on fractured specimens.

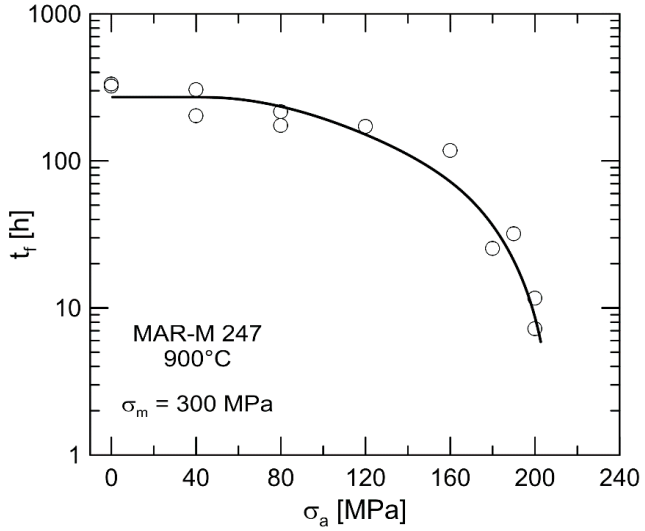

Fig. 3. Influence of superimposed stress amplitude σ_a on the mean stress σ_m = 300 MPa on the time to fracture t_f at 900 °C.

The fracture surface of the specimen loaded by mean stress σ_m = 300 MPa without superimposed stress amplitude σ_a, i.e. by pure creep, is shown in Fig. 4 (a). The crack initiated and propagated intergranularly along the grain boundaries and interdendritic areas, which is a characteristic feature of the creep crack growth, described e.g. by Reed (2008) and Matan et al. (1999). Numerous carbides were observed on the fracture surface, acting as a brittle phase and favorable sites for the crack initiation. Multiple crack initiation was observed on the fracture surface. One example of the initiation site is shown in detail in Fig. 4 (a).

In Fig. 4 (b) is shown the fracture surface of the specimen after creep/fatigue test, particularly loaded by σ_m = 300 MPa and the stress amplitude σ_a = 40 MPa. The crack initiation and early stages of the crack propagation

were intergranular along interdendritic areas, which is characteristic for pure creep. When the crack, once formed by the creep mechanism, reached a specific length the crack propagation mechanism changed to the transgranular. The fatigue cracks start to propagate from the creep cracks. They can be considered as structural defects, acting as the stress concentration sites, which cause the cyclic strain localization and further crack propagation by fatigue mechanism. From the point of view of the time to fracture, the dominating damage is, however, the creep damage. The lifetime of the specimen is thus similar to the specimen loaded only by the mean stress. Because no striations were detected on the fracture surface created by the fatigue growth, it can be concluded that the fatigue cracks grew with a very low rate.

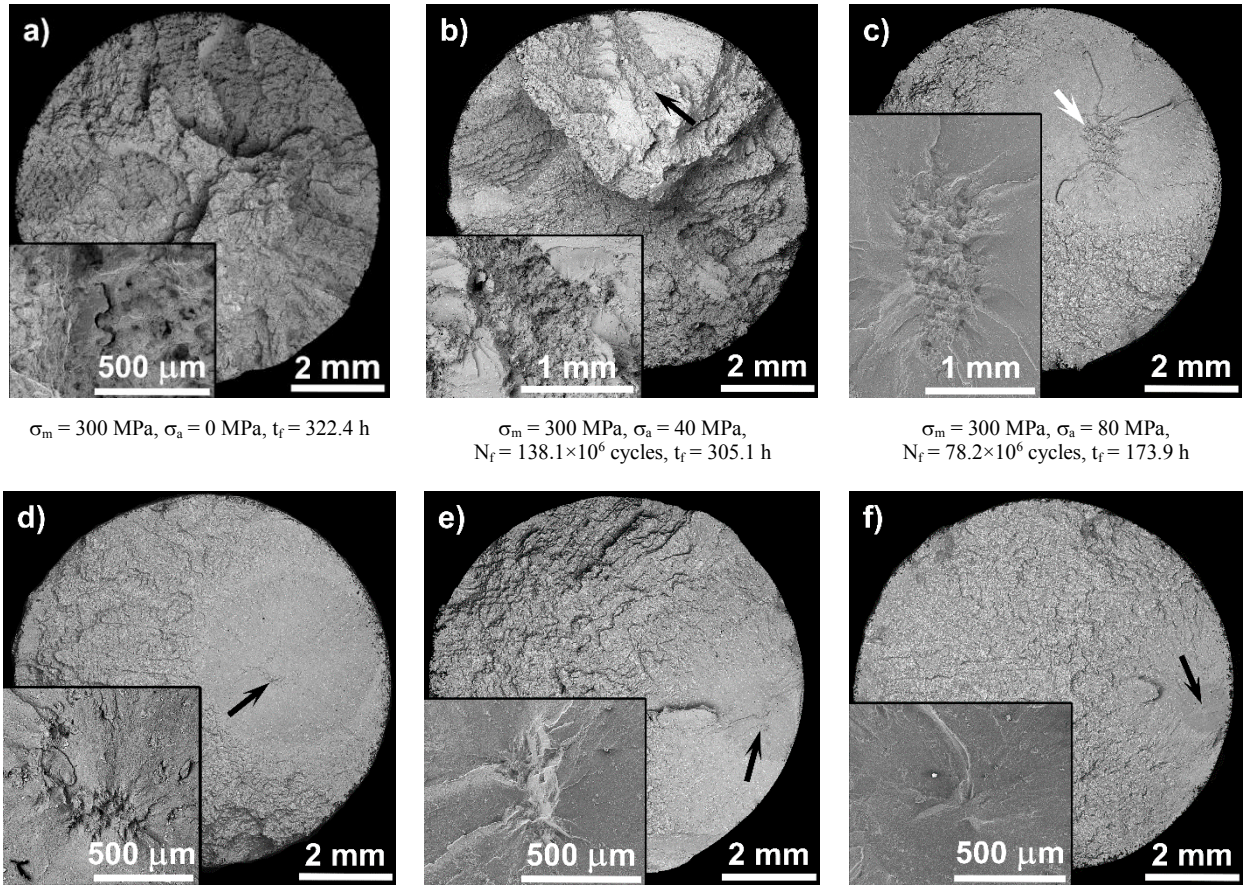

σ_m = 300 MPa, σ_a = 0 MPa, t_f = 322.4 h

σ_m = 300 MPa, σ_a = 40 MPa, $N_f = 138.1\times10^6$ cycles, t_f = 305.1 h

σ_m = 300 MPa, σ_a = 80 MPa, $N_f = 78.2\times10^6$ cycles, t_f = 173.9 h

σ_m = 300 MPa, σ_a = 120 MPa, $N_f = 74.0\times10^6$ cycles, t_f = 171.8 h

σ_m = 300 MPa, σ_a = 160 MPa, $N_f = 50.7\times10^6$ cycles, t_f = 117.8 h

σ_m = 300 MPa, σ_a = 200 MPa, $N_f = 3.0\times10^6$ cycles, t_f = 7.2 h

Fig. 4. Fracture surfaces of specimens tested under creep/fatigue loading.

Increase of the stress amplitude to σ_a = 80 MPa led to a significant decrease of time to fracture (Fig. 3). The specimen had nearly twice shorter lifetime when compared to the tests with the stress amplitudes 40 MPa. The crack initiation occurred in the interior of the specimen, Fig. 4 (c). The crack initiation site is marked by an arrow. The fracture surface is featured with a typical fish eye. The initial area of the crack growth can be characterized as interdendritic area with dominant creep damage processes. Due to higher stress amplitude, the role of fatigue loading becomes more significant and the growth of the fatigue crack in propagation stage II have become decisive for the lifetime. The fatigue crack propagated perpendicularly to the loading axis. The striations, typical for the fatigue crack growth at higher rates, were observed on the fracture surface. No evidence of the crystallographic crack propagation was observed on the specimen fracture surface.

The similar appearance of the fracture surface was observed on specimen loaded by mean stress and stress amplitude σ_a = 120 MPa, see Fig. 4 (d). Also, in this case, the fish eye on the fracture surface was present. The size of the creep damage-driven crack initiation site situated in interdendritic area is four times smaller than in Fig. 4 (c). The first occurrence of the crystallographic crack propagation in a limited area (the size of the largest facet is 60 μm) was found in the vicinity of the crack initiation site by careful observation of the fracture surface. Subsequently, the crack propagates in stage II, perpendicularly to the loading axis. It is important to note that the influence of creep cannot be neglected even in stage II crack propagation because the defects originating from creep damage act as suitable fatigue crack path.

Fracture surface of the specimen loaded by mean stress and stress amplitude σ_a = 160 MPa is shown in Fig. 4 (e). The crack initiation site, shown in the detail in Fig. 4 (e), documents the interaction of creep/fatigue damage mechanism. The areas of interdendritic crack propagation (size about 150 μm) created as a consequence of the creep damage are connected by a facet, arising from the fatigue damage (size around 500 μm). The effect of creep damage is still notable, also during stage II crack propagation.

The dominance of the fatigue damage mechanism was observed on the fracture surface after creep/fatigue test with stress amplitude σ_a = 200 MPa, see Fig. 4 (f). The crack was initiated by formation of crystallographic facets, from which finally grew the magistral fatigue crack. A facet of 170 μm in size, at the crack initiation site in the middle of the fish eye documents this behavior. No evidence of the creep damage at the crack initiation site was found.

In Fig. 5 is shown a typical fracture surface after fully reverse (R = -1) fatigue loading at 900 °C. The fatigue crack initiation was in this case on the surface of the specimen and the crack propagation was predominantly in crystallographically dependent stage I regime, characteristic for nickel-based superalloy, a typical low stacking fault energy material. This phenomenon was reported in several studies on different alloys, e.g. Šmíd et al. (2016), MacLachlan and Knowles (2001).

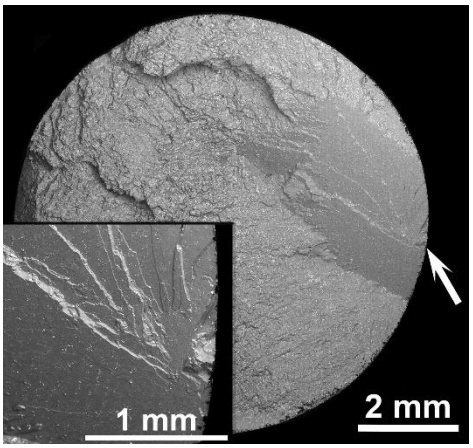

σ_m = 0 MPa, σ_a = 280 MPa, $N_f = 0.915 \times 10^6$ cycles, t_f = 2.2 h

Fig. 5. Fracture surface of specimen after fully reverse loading at 900 °C.

4. Conclusions

The high-frequency stress amplitudes superimposed on mean stress σ_m = 300 MPa at the temperature 900 °C do not influence the time to fracture of MAR-M 247 processed by HIP until reaching a threshold value. The threshold value was identified to be about 60 MPa for the studied material and applied σ_m. The contribution of creep or fatigue damage mechanism on final failure based on analysis of fracture surfaces can be summarized as follows:

- Interaction of the creep/fatigue damage mechanism was observed for stress amplitudes in the range 40 - 160 MPa. The crack initiation was caused by creep damage and formation of early creep cracks. The

fatigue cracks initiate from this damage and propagate in non-crystallographic way in stage II crack growth. In the stress amplitude range 40 - 120 MPa it was observed, that the size of the creep cracks necessary for initiation of fatigue cracks decreases with increasing stress amplitude. Moreover, with increasing stress amplitude the fatigue crack growth rate increases. Both effects result in lifetime decrease with increasing stress amplitude.

- The effect of initiation and propagation of fatigue cracks on the lifetime measurably prevails above the stress amplitude 60 MPa.
- Application of stress amplitudes above 160 MPa, changes the initiation mechanism in such a way, that the crystallographic facets develop and serve as the initiation sites for the final fatigue crack which propagates in stage II. The fish eye, a typical fracture surface feature, was observed for the stress amplitudes above 80 MPa.
- The fatigue damage mechanism was dominant from the stress amplitudes of 200 MPa. The fatigue crack initiation was mainly crystallographic by facets while the crack propagation was non-crystallographic.
- Fully reversed cyclic loading (zero mean stress), i.e. pure fatigue, results in crystallographic crack initiation on the specimen surface.

Acknowledgements

This research was financially supported by the project CZ.01.1.02/0.0/0.0/15_019/0004399 of Ministry of Industry and Trade of the Czech Republic and by the project of Ministry of Education, Youth and Sports of the Czech Republic m-IPMinfra (CZ.02.1.01/0.0/0.0/16_013/0001823). The base research infrastructure IPMinfra was used for the experimental work.

References

Beck, T., Ratchev, R., Moalla, M., Lang, K. H., Löhe, D., Rémy, L., Petit, J.,2002. Lifetime, cyclic deformation and damage behaviour of MAR-M-247 CC Under in-Phase, out-of-Phase and phase-Shift TMF-Loadings, in European Structural Integrity Society. Elsevier. p. 115-124.

Goswami, T., Hanninen, H., 2001. Dwell effects on high temperature fatigue behavior Part I. Materials & Design. 22(3): p. 199-215.

Goswami, T., Hanninen, H., 2001. Dwell effects on high temperature fatigue damage mechanisms Part II. Materials & Design. 22(3): p. 217-236.

Horník, V., Šmíd, M., Hutař, P., Kunz, L., Hrbáček, K., 2017. Interaction of creep and high cycle fatigue of IN 713LC superalloy. Solid State Phenomena. Vol. 258 SSP. 595-598.

Kunz, L., Horník, V., Hutař, P., Fintová, S., 2017. Initiation of fatigue cracks and lifetime of Ni-base superalloys at high mean stress and temperature. Procedia Structural Integrity. 7: p. 44-49.

Lukáš, P., Kunz. L., Svoboda, J., 1997. Retardation of creep in <001>/oriented superalloy CMSX-4 single crystals by superimposed cyclic stress. Mat. Sci. Eng. A234-236, 459-462.

MacLachlan, D. W., Knowles, D. M., 2001. Fatigue behaviour and lifing of two single crystal superalloys. Fatigue and Fracture of Engineering Materials and Structures. 24(8): p. 503-521.

Matan, N., Cox, D. C., Carter, P., Rist, M. A., Rae, C. M. F., Reed, R. C., 1999. Creep of CMSX-4 superalloy single crystals: effects of misorientation and temperature. Acta Materialia. 47(5): p. 1549-1563.

Reed, R.C., 2008. The Superalloys: Fundamentals and Applications. Cambridge University Press.

Šmíd, M., Horník, V., Hutař, P., Hrbáček K., Kunz, L., 2016. High Cycle Fatigue Damage Mechanisms of MAR-M 247 Superalloy at High Temperatures. Trans Indian Inst. Met. 69, 393 – 397.

Šulák, I., Obrtlík, K., 2017. Effect of tensile dwell on high-temperature low-cycle fatigue and fracture behaviour of cast superalloy MAR-M247. Engineering Fracture Mechanics. 185: p. 92-100.